ACS APPLIED MATERIALS & INTERFACES

Research Article

www.acsami.org

Polypropylene/Glass Fiber Hierarchical Composites Incorporating Inorganic Fullerene-like Nanoparticles for Advanced Technological Applications

Ana M. Díez-Pascual*,† and Mohammed Naffakh‡

†Instituto de Ciencia y Tecnología de Polímeros (ICTP-CSIC), Juan de la Cierva 3, 28006 Madrid, Spain

‡Departamento de Ingeniería y Ciencia de los Materiales, Escuela Técnica Superior de Ingenieros Industriales, Universidad Politécnica de Madrid, José Gutiérrez Abascal 2, 28006 Madrid, Spain

Supporting Information

ABSTRACT: Novel isotactic polypropylene (iPP)/glass fiber (GF) laminates reinforced with inorganic fullerene-like tungsten disulfide (IF-WS_2) nanoparticles as environmentally friendly fillers have been successfully fabricated by simple melt-blending and fiber impregnation in a hot-press without the addition of any compatibilizer. The influence of IF-WS_2 concentration on the morphology, viscosity. and thermal and mechanical behavior of the hierarchical composites has been investigated. Results revealed an unprecedented 62 °C increase in the degradation temperature of iPP/GF upon addition of only 4.0 wt % IF-WS_2. The coexistence of both micro- and nanoscale fillers resulted in synergistic effects on enhancing the stiffness, strength, crystallinity, thermal stability, glass transition (T_g) and heat distortion temperature (HDT) of the matrix. The approach used in this work is an efficient, versatile, scalable and economic strategy to improve the mechanical and thermal behavior of GF-reinforced thermoplastics with a view to extend their use in advanced technological applications. This new type of composite materials shows great potential to improve the efficiency and sustainability of many forms of transport.

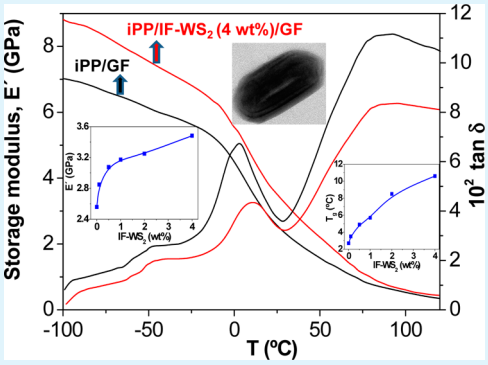

KEYWORDS: *hierarchical composites, polypropylene, inorganic fullerene-like nanoparticles, thermal properties, mechanical performance*

1. INTRODUCTION

Semicrystalline thermoplastics such as polyamide (PA), polyphenylene sulphide (PPS) and poly(ether ether ketone) (PEEK) are usually reinforced with high modulus fibers in order to enhance their mechanical and thermomechanical performance for cost-effective replacement of conventional engineering materials in demanding applications like automotive, aeronautical, marine, electronics, etc.[1,2] One of the few commodity polymers that can be efficiently fiber reinforced for structural applications is polypropylene (PP), due to its well-balanced physical and mechanical properties, low density, easy processability, and low cost.[3] Nevertheless, because of the nonpolar and chemically inert nature of PP, the polymer-fiber interfacial adhesion is typically weak, which results in poor mechanical performance. To overcome this drawback, researchers have frequently employed interfacial compatibilizers such as maleic anhydride-grafted PP (MAH-g-PP).[4] Mohanty et al.[5] studied the effect of MAH-g-PP on the interfacial properties of PP/fiber composites. The PP part of the grafted system is compatible with the matrix, whereas the anhydride part reacts with the fiber, thereby leading to a favorable interface. The role of glycidyl methacrylate (GMA) as an interfacial modifier has also been examined.[6]

On the other hand, a wide number of nanoscale fillers including montmorillonite clays,[7] $CaCO_3$,[8] SiO_2,[9] carbon nitrides,[10] and carbon nanotubes (CNTs)[11,12] have been incorporated into PP to improve its mechanical performance and simultaneously increase its longevity and durability, thus fulfilling the requirements for certain engineering applications. The efficiency of these nanofillers on enhancing the physical properties of PP depends strongly on the filler concentration, size, shape, aspect ratio, surface characteristics and degree of dispersion. Generally, the nanofillers improve the matrix stiffness and strength thought lead to decreases in impact strength and ductility induced by agglomeration, stress concentration, and confinement effects on polymer chain mobility. Therefore, a lot of efforts have been recently focused on the design of novel strategies to prepare nanocomposites with optimal filler dispersion. Meng and Dou[13] grafted pimelic acid onto the surface of $CaCO_3$ nanoparticles to attain a uniform distribution and enhance the matrix toughness. Gao et al.[14] prepared PP/nano-$CaCO_3$ blends via low-frequency-vibration injection molding to improve the structure and

Received: July 10, 2013
Accepted: September 9, 2013
Published: September 9, 2013

   dx.doi.org/10.1021/am402750t | ACS Appl. Mater. Interfaces 2013, 5, 9691−9700

mechanical properties of the resulting nanocomposites. Altan et al.[15] incorporated TiO_2 and ZnO nanoparticles coated with MAH-grafted styrene ethylene butylene styrene (MAH-g-SEBS) and silane, respectively, in a PP matrix to obtain better surface adhesion and finer dispersion. Inorganic nanoparticles of layered metal dichalcogenides such as WS_2 and MoS_2[16] show great potential as reinforcement for polymer composites. These noncarbon materials possess similar structure to fullerenes, and are named inorganic fullerene-like (IF) nanoparticles. They have exceptional properties such as very high stiffness and strength, attributed to their small size (typically in the range of 40−180 nm), quasi-spherical shape, closed-cage layered structure and chemical inertness. Moreover, they have excellent solid lubricant behavior and display low agglomerating tendency, and hence can be homogenously dispersed within polymer matrices via simple melt-blending technique.[17,18] Additionally, they are cheaper and easier to synthesize than organic nanofillers (i.e., CNTs, nanofibers, graphene), less flammable, biocompatible, and nontoxic.

Conventional glass fiber-reinforced polymers (GFRPs) have been developed over the past half-century to provide a wide range of materials that combine superior mechanical properties and lightweight with chemical and environmental resistance.[19] However, the use of these composites is usually hindered by poor fracture toughness, compression and interlaminar properties. To address these issues, additional nanoscale fillers including CNTs[20,21] or clays[22] have been mixed with GFs to develop hierarchical (also named hybrid or multiscale) composites. In particular, the incorporation of nanoclays to GFRPs has been reported to improve significantly the heat distortion temperature, flexural and impact strengths.[22] The synergistic effect of GFs with the inorganic particles is supposed to be the main reason for the observed mechanical enhancements. Nonetheless, these hierarchical composites constitute complex systems, and there is to date very scarce information available about the phenomena behind the property changes upon addition of inorganic nanofillers to fiber-reinforced thermoplastics. Recently, Cui et al.[23] functionalized nano-ZnO nanoparticles with a silane coupling agent, which were subsequently mixed with PP/MAH-g-PP/GF to develop hybrid materials with improved mechanical performance. The disadvantage of their approach is the large number of processing stages, which makes it difficult to scale up and hence limits its potential industrial applications.

The aim of the current study is to show the advantages of using IF-WS_2 as a suitable nanoreinforcement for enhancing the performance of conventional isotactic polypropylene (iPP)/GF laminates. The hierarchical composites were prepared through an environmentally friendly and scalable procedure involving melt-blending and hot-press processing stages, without the aid of any modifier or compatibilizing agent. The influence of the nanoparticle concentration on the morphology, melt viscosity, mechanical and thermal properties including tensile, flexural, interlaminar shear, dynamic mechanical, heat distortion temperature, crystallization behavior, thermal stability, and thermal conductivity is analyzed.

2. EXPERIMENTAL SECTION

Materials. iPP was supplied by Repsol-YPF (Spain), with 95% isotacticity, a viscosity average molecular weight of 179,000 g/mol, a density of 0.92 g/cm^3 and a polydispersity of 4.77. Inorganic fullerene-like tungsten disulfide (IF-WS_2) nanoparticles (NanoLub, $d_{25\ °C} \approx 7.5$ g/cm^3) were provided by Nanomaterials (Israel). They exhibit a quasi-spherical shape with an average aspect ratio of 1.4 and a mean diameter of 80 nm. E-glass fiber woven fabric (HexForce^R 00791, twill 2/2), with an areal density of 290 g/m^2 and thickness of 0.25 mm, was provided by Hexcel (France).

Preparation of iPP/IF-WS_2/GF Composites. Prior to compounding, all the components were placed in an oven at 100 °C for 24 h to remove absorbed moisture. After drying, iPP was physically mixed with different concentrations of IF-WS_2 (0.1, 0.5. 1.0, 2.0, and 4.0 wt %) in a Haake Rheocord 90 extruder operating at 210 °C, with mixing times of 10 min and a rotor speed of 150 rpm. The extrudate was then used to prepare films with a thickness of ∼0.5 mm by compression molding with a hot-press at 210 °C under successive pressure dwells of 5, 40, and 130 bar, for periods of 6 min at each pressure.

The laminates were prepared by the film-stacking process. Four layers of GF were alternatively stacked within five iPP/IF-WS_2 films in a closed mold. Consolidation of the material was made at 210 °C in a hot-press. A three-step pressure profile (5, 30, and 120 bar) was applied to improve fiber impregnation. The heating rate to the dwell temperature was ∼5 °C/min, and the cooling to room temperature was carried out at a rate ≤3 °C/min. The resulting laminates had a fiber weight fraction of 34 ± 1%, a nominal thickness of 1.2 ± 0.1 mm and an average void content <2% (estimated by density measurements). Prior to characterization, they were cut into test specimens with a Rockwell Delta band saw. For comparative purposes, neat iPP and the binary iPP/IF-WS_2 nanocomposites were also characterized.

Materials Characterization. Scanning electron microscopy (SEM) images were obtained with an SU8000 Hitachi scanning electron microscope to investigate the extent of fiber impregnation and the distribution of the nanoparticles within the composites. Samples were prepared by sequentially polishing the observation surfaces with 240, 320, 400, 600, 800, and 1200 grit silicon carbide paper followed by a 3 μm diamond abrasive and a 0.05 μm colloidal silica suspension. Prior to examination, specimens were coated with a ∼5 nm Au/Pd overlayer to render conductive the sample surface.

Dynamic shear viscosities were obtained with a rheometer (AR 1000, TA Instruments) using a parallel plate system (25 mm diameter and 0.75 mm gap). Samples were tested at 200 °C, under nitrogen conditions, after drying under vacuum at 100 °C to completely remove moisture. Frequency sweeps from 0.02 to 500 rad/s were performed within the linear viscoelastic region of the materials. Rheological tests were carried out in triplicate to ensure repeatability.

The heat distortion temperature (HDT), temperature at which the material deflects by 0.25 mm at an applied force, was measured in a three-point bending mode using a HDT/VICAT heat deflection tester according to ASTM D648 standard. Specimens were conditioned at 23 ± 2 °C and 50 ± 5% RH for 40 h prior to the tests. The sample position was edgewise, test span 100 mm, the surface stress 1.8 MPa and the heating rate 2 °C/min.

Thermal conductivity experiments were performed with a KES-F7 Thermo Labo type II device equipped with a temperature controlled hot plate and placed in a thermostatic chamber to be kept in a constant operating environment. The effect of the contact thermal resistance was removed by measuring the thermal conductivity of a reference material. The in-plane (K_x) and transverse (K_z) thermal conductivities were determined by measuring the heat flux and the differential temperature across the samples. Five specimens for each laminate were tested and the average value is reported.

Differential scanning calorimetry (DSC) measurements were carried out on a differential scanning calorimeter (Q-100, TA Instruments) under a nitrogen atmosphere using standard aluminum pans. Samples of ∼10 mg were exposed to the following temperature scans: heating to 210 °C at a rate of 10 °C/min, holding at this temperature for 5 min to erase thermal history effects and then cooling to 30 °C at a scan rate of 10 °C/min. The melting temperature (T_m) was taken as the maximum of the endothermic peak appearing on the heating scans while the crystallization temperature (T_c) was determined as the minimum of the exothermic peak on the cooling thermograms. The degree of crystallinity (X_c) was estimated according to the relation: $X_c = \Delta H_m/(\Delta H^\circ_m w_m)$, where ΔH°_m is the heat of fusion for a 100%

crystalline iPP taken as 177 J/g [18], ΔH_m is the apparent melting enthalpy and w_m the weight fraction of the matrix.

Thermogravimetric analysis (TGA) experiments were conducted on a thermobalance (Q-500, TA Instruments) at a heating rate of 10 °C/min. The temperature was scanned from 100 to 850 °C under a nitrogen atmosphere. Measurements were performed on samples of ~20 mg with a purge gas flow rate of 50 mL/min.

Quasi-static mechanical tests were carried out on a servo-hydraulic testing machine (type MTS 858) equipped with a temperature control system, at a constant crosshead speed of 1 mm/min and a load cell of 100 kN. Tensile, flexural and interlaminar shear tests were performed according to the ASTM D638, D790 and D2344 standards, respectively. Specimens were conditioned at 23 ± 2 °C and 50 ± 5% RH for 24 h prior to the measurements. Five specimens for each laminate were tested, and the mean values with the standard deviations are reported.

Dynamic mechanical analysis (DMA) experiments were performed in dual cantilever mode with a TA Instruments Q-800 dynamic-mechanical analyzer. Measurements were performed over the temperature range between −100 and 120 °C, at a heating rate of 3 °C/min and a constant frequency of 1 Hz, under a nitrogen flow rate of 20 mL/min.

3. RESULTS AND DISCUSSION

Melt Viscosity and Morphology. The study of the rheological behavior of polymeric materials in the molten state is crucial from both processing and performance points of view to understand internal microstructural changes, structure property relationships and optimize processing conditions. The melt viscosity (η) of iPP/IF-WS_2/GF laminates at 200 °C as a function of frequency ω is depicted in Figure 1. For comparison, data of neat iPP are also included. As can be observed, η of iPP/GF laminate is slightly higher than that of neat iPP due to the increased resistance to shear flow caused by the confinement of the polymer chains within the reinforcing fibers, in agreement with results reported for short-GF reinforced iPP composites.[24] The viscosity of all the samples decreases with increasing frequency, showing non-Newtonian behavior. This reduction is more pronounced for the laminates with higher nanoparticle contents, indicating strong shear thinning character, and the onset for this behavior is shifted to smaller frequencies, thus longer relaxation times, upon addition of the nanoparticles. Moreover, all the hybrids exhibit lower η than iPP/GF over the frequency range studied, and the decrease becomes more significant with increasing IF-WS_2 concentration. For example, at ω = 1 rad/s (inset of Figure 1), η of iPP/GF dropped by about 19 and 71% when 0.1 and 4.0 wt % IF-WS_2 were added, respectively. Similar behavior of melt viscosity reduction was reported for silica-reinforced poly(ethylene 2,6-naphthalate) (PEN)[25] and poly(ethylene terephthalate) (PET)[26] nanocomposites. Romero-Guzman et al.[27] dealing with polystyrene (PS)/POSS-styrene blends also found a decrease in matrix viscosity with increasing nanofiller content attributed to a plasticizing effect of the nanoparticles that increased the free volume and reduced the entanglement density. To elucidate whether the viscosity diminution observed here is related to a change in free volume due to the addition of the nanoparticles, the increase in fractional free volume (f) within the melt polymer matrix was roughly estimated by $\sim 3V_f\Delta/a$,[28] where V_f is the particle volume fraction, a the average particle radius and Δ the thickness of the excluded volume layer around each nanoparticle. Thus, taking Δ = 0.1 nm, the increase in free volume would be between 1.5×10^{-7} and 3.0×10^{-6} for the range of volume fractions investigated, which is lower than 0.01% rise for a typical f in the molten state.[28] Therefore, the effect of free volume on the viscosity is expected to be negligible.

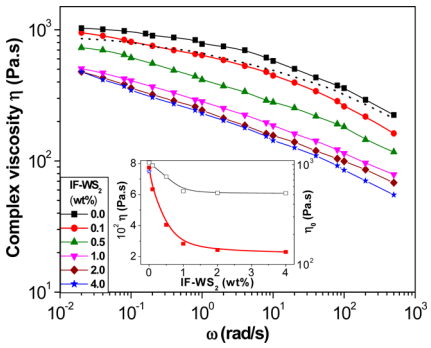

Figure 1. Complex viscosity η at 200 °C as a function of frequency ω for iPP/IF-WS_2/GF laminates. Data for neat iPP are shown as a dotted black line. The inset displays the evolution of η at ω = 1 rad/s (solid red squares) and the zero-shear viscosity, η_0 (empty black squares) vs nanoparticle loading, and the blue star corresponds to η_0 value for neat iPP.

The rheological behavior of polymer melts in the terminal zone can be characterized by parameters such as the zero-shear viscosity (η_0), which can be obtained by fitting η values using the Carreau-Yasuda model,[29] and the results for the different laminates and neat iPP are displayed in the inset of Figure 1. A decrease in η_0 is observed upon increasing IF-WS_2 concentration up to 1.0 wt % loading, and remains approximately unchanged at higher contents, results that are in contrast to classical predictions for hard-sphere-filled suspensions which expect a monotonic rise with increasing particle concentration.[30] This fall in η_0 is attributed to slippage between the matrix and the quasi-spherical nanoparticles with a smooth nonporous surface, which serve as ball-bearing agents, reducing the coefficient of friction[31] and facilitating the flow of the polymer chains. This enables an optimal fiber impregnation during the hot-press processing, as revealed by SEM micrographs of the laminates. Representative images taken from the cross section of iPP/IF-WS_2 (2.0 wt %)/GF are displayed in Figure 2. The matrix had uniformly penetrated within the GF tows, and no voids were detected around the fibers, indicative of a good GF-resin interfacial adhesion. Further, none of the laminates exhibited microcracks, undulations, local fiber wrinkles or delamination, attesting to their good quality. This corroborates that the IF-WS_2 acted as solid lubricants when the iPP/nanoparticle mixture was exposed to high shear forces and

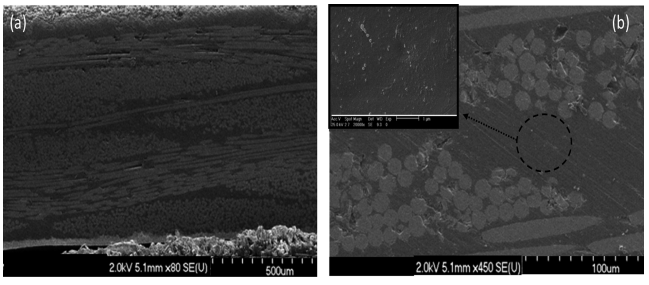

Figure 2. SEM images at different magnifications obtained from the cross section of iPP/IF-WS_2 (2.0 wt %)/GF laminate. The inset in b shows the IF-WS_2 nanoparticles randomly distributed within the matrix.

heat during the melt-blending process, leading to a very uniform nanofiller dispersion within the matrix, as shown in the high magnification image obtained from a matrix rich region between fiber tows (inset in Figure 2b). The IF-WS_2 (bright spots) are found to be randomly dispersed throughout the iPP matrix, and exhibit quasi-spherical shape with an average diameter of 85 nm, in agreement with the value for as-received particles. Interestingly, the phenomenon of viscosity reduction observed upon addition of the IF-WS_2 is in contrast with the typical behavior found for iPP nanocomposites such as those reinforced with CNTs[32] or ZnO nanoparticles,[33] where η rises with increasing nanofiller loading. The formation of a highly entangled interconnected CNT structure[32] or the increase in the number of frictional interactions between the nanoparticles and the matrix[33] are believed to be the reasons for the reported viscosity increments. A rise in matrix viscosity could cause poor wetting/interpenetration of the glass fibres leading to weak GF-matrix adhesion during the laminate fabrication stage.[23] An in-depth rheological study will be undertaken to fully explain the mechanisms of viscosity reduction by the IF-WS_2 and will be reported elsewhere.

Thermal Properties. The crystallization process plays a crucial role on the properties of semicrystalline polymers; therefore, it is important to analyze the influence of the IF-WS_2 on the crystallization behavior of iPP/GF (Figure 3). The

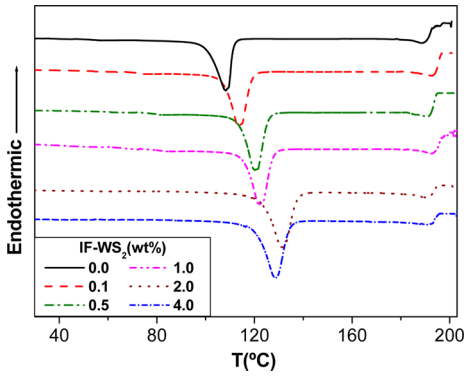

Figure 3. DSC cooling scans of iPP/IF-WS_2/GF laminates from the melt to room temperature at a rate of 10 °C/min.

thermal data obtained from DSC analysis of the different laminates such as crystallization temperature (T_c), melting temperature (T_m) and degree of crystallinity (X_c) are summarized in Table 1. T_c of iPP/GF is 107 °C, similar to

Table 1. Thermal Parameters Obtained from DSC and TGA analysis of iPP/IF-WS_2/GF Laminates[a]

IF-WS_2 content (wt%)	T_c (°C)	T_m (°C)	X_c (%)	T_i (°C)	T_{10} (°C)	T_{max} (°C)	OI (%)
0.0	107	163	50.4	379	454	505	31.6
0.1	114	163	51.3	405	463	509	31.7
i0.5	119	164	52.5	417	468	516	31.9
1.0	122	165	54.9	425	476	522	32.4
2.0	131	164	57.2	426	482	524	33.0
4.0	129	165	56.8	441	490	530	33.9

[a] T_m, melting temperature; T_c, crystallization temperature; X_c, degree of crystallinity; T_i, initial degradation temperature obtained at 2% weight loss; T_{10}, temperature for 10% weight loss; T_{max}, temperature of maximum rate of weight loss; OI, oxygen index parameter.

that of neat iPP,[18] which implies that the inclusion of GFs is not effective in promoting the crystallization of the polymer. In contrast, the addition of increasing nanoparticle contents provokes a rise in both T_c and X_c, indicating that the IF-WS_2 are efficiently acting as nucleating agents for the iPP matrix, facilitating the crystallization of the molecular chains and increasing the crystallization rate. The increases observed (up to 22 °C in T_c and 6% in X_c at 4.0 wt % IF-WS_2) are larger than those found for binary iPP/IF-WS_2 nanocomposites,[18] hinting toward the existence of a synergistic effect of both fillers on accelerating the crystallization of iPP, thereby making it crystallize at higher temperature, which will shorten the molding cycle in practical production. This is consistent with the behavior reported for PP/ZnO/GF[23] and PP/SiO_2/GF hybrids,[34] where the combination of nano and microfillers further increased the T_c of the matrix, albeit the increments attained in the above-mentioned systems (~7 and 6 °C at 2.0 wt % ZnO and 1.0 wt % SiO_2 content, respectively) are smaller than those found for the same amount of IF-WS_2. Further, X_c of PP decreased upon incorporation of ZnO or SiO_2 and GF, while the combined nucleating effect of IF-WS_2/GF resulted in a slight raise in crystallinity. On the other hand, T_m of iPP/GF (163 °C) is slightly lower than that reported for the pure matrix,[18] and remains merely unaffected upon addition of the IF-WS_2, in agreement with the trend found for ZnO[23] and SiO_2[34] modified-PP/GF composites.

The room temperature thermal conductivity of the iPP based laminates was measured both in the transverse (K_z) and in-plane (K_x) directions, and the results are shown in Figure 4.

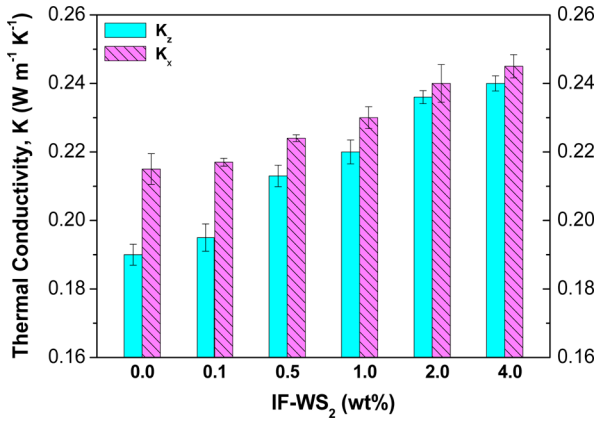

Figure 4. Transverse (K_z) and in-plane (K_x) thermal conductivity for iPP/IF-WS_2/GF laminates.

Only slight anisotropy in thermal conductivity was detected, being K_z in all cases lower than K_x. Thus, the orthotropic ratio (K_x/K_z) ranges from ~1.2 for iPP/GF to ~1 for iPP/IF-WS_2 (4.0 wt %)/GF. The observed orthotropy for the reference laminate is the result of the alignment of the glass fibers in-plane, as previously reported for other thermoplastic/GF composites.[20] The very small degree of anisotropy found for the hybrid systems confirms the isotropic distribution of the IF-WS_2 nanoparticles, as revealed by SEM analysis. This behavior is in contrast to that described for hierarchical GF-reinforced laminates incorporating CNTs[21,35] where strong anisotropy in K was detected, ascribed to the alignment of the CNTs along the resin flow direction during processing.

K_z and K_x of iPP/GF are about 0.19 and 0.22 W m^{-1} K^{-1}, respectively, slightly smaller than the thermal conductivity

dx.doi.org/10.1021/am402750t | ACS Appl. Mater. Interfaces 2013, 5, 9691−9700

measured for neat iPP (~0.24 W m^{-1} K^{-1}), because the GF fabric has a low K[21] (around 0.05 W m^{-1} K^{-1}). The incorporation of the IF-WS_2, which exhibit about twice the thermal conductivity of the neat matrix,[36] results in significant K_z and K_x increments, up to 26 and 14%, respectively, at 4.0 wt % nanoparticle content. Interestingly, the rise in K_z is significantly larger than that in K_x for all the laminates, which can be explained considering that the nanoparticles have more influence in the transverse properties, which are matrix dominated, while only affect slightly the in-plane properties that are more fiber dominated. Analogous trend has been reported for PEEK/CNT/GF laminates,[20] where K_z increased by ~48% at 1.0 wt % CNT loading while the rise in K_x was only around 18%. Albeit very few studies have reported the thermal conductivity of hierarchical laminates, particularly those based on a thermoplastic polymer,[20,21,37] it is worthy to note that for the same nanofiller concentration, the increases in K_z of the matrix attained upon addition of CNTs are only about double those achieved in this work, whereas much higher differences would be expected taking into account the extraordinary high thermal conductivity of CNTs.[38] The strong agglomerating tendency of CNTs, the small thermal conductance of the nanotube-polymer interface and the high interfacial thermal resistance between nanotubes within a bundle should restrict the heat transfer, thereby limiting the property enhancement, whereas for composites incorporating IF-WS_2 the large nanofiller−matrix interfacial contact area and the very homogeneous dispersion lead to experimental K values even higher than the theoretical predictions.

The thermal stability of iPP/IF-WS_2/GF laminates was investigated using TGA, and typical thermograms under a nitrogen atmosphere are presented in Figure 5. The character-

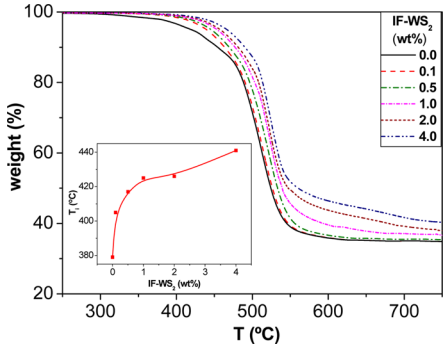

Figure 5. TGA curves under nitrogen atmosphere for iPP/IF-WS_2/GF laminates in the temperature range between 250 and 750 °C. The inset displays the initial degradation temperature T_i vs nanoparticle content.

istic degradation temperatures for the different laminates including the initial degradation temperature (T_i), the temperature of 10% weight loss (T_{10}) and the temperature of maximum rate of weight loss (T_{max}) are collected in Table 1. All the samples exhibit a single decomposition stage, similar to that found for neat iPP,[18] indicating that the random scission of the polymeric chains is the predominant degradation process. T_i of iPP/GF is around 36 °C higher than that of the neat matrix, and rises gradually with increasing IF-WS_2 loading, since these nanoparticles are thermally stable in nitrogen up to 800 °C. Thus, the increments in T_i in comparison to the reference laminate are about 26, 38, 46, 47, and 62 °C for IF-WS_2 contents of 0.1, 0.5, 1.0, 2.0, and 4.0 wt %, respectively. A similar trend is found for T_{max}, albeit the increases are smaller. It is worthy to note that these thermal stability enhancements are considerably larger than those found for binary iPP/IF-WS_2 nanocomposites,[18] probably arising from the combined effect of the nano- and micro- fillers. Thus, both the IF-WS_2 and the GFs can act as barriers that effectively hinder the transport of volatile decomposed products from the bulk of the polymer to the gas phase, hence decelerating the decomposition process. Upon increasing nanoparticle content, the barrier effect becomes stronger, which is reflected in higher degradation temperatures. Another factor that contributes to the thermal stability improvement is the rise in thermal conductivity, as discussed previously, which facilitates the heat dissipation from the inner of the sample to the surface. Analogous behavior of thermal stability increase has been reported for PP/GF composites reinforced with other inorganic nanoparticles such as clays.[39] Nonetheless, the amount of nanofiller required to attain a certain rise in the degradation temperatures of the matrix is smaller in the case of IF-WS_2, hinting toward a more effective heat barrier effect of these nanoparticles probably induced by their more homogeneous dispersion and spherical shape, and hence larger specific surface area.

The IF-WS_2 not only enhance the overall thermal stability of the hybrid laminates, but also promote stable char formation. The char residues under inert atmosphere have a very important implication in the flame retardant ability of the materials since they can be correlated with the Oxygen Index (OI) through the equation developed by D. W. van Krevelen:[40] OI × 100 = 17.5 + 0.4 CR, where CR is the char residue in wt% at 850 °C. The limiting OI is defined as the minimum amount of oxygen in a nitrogen−oxygen mixture that is just sufficient to maintain combustion after ignition. A material is considered flammable when OI ≤ 26%. Because of its wholly aliphatic hydrocarbon structure, iPP burns very rapidly with a relatively smoke-free flame and without leaving a char residue, hence has a high flammability. The incorporation of 34 wt % GF improves the fire performance of this polymer, leading to an OI of 31.6% (Table 1). Upon addition of increasing amounts of the IF-WS_2, the OI progressively rises, reaching 33.9% at 4.0 wt % loading. The results reveal a synergistic improvement in flame retardancy compared with the binary iPP/IF-WS_2 nanocomposites;[18] similar synergistic enhancements have been reported for other ternary systems like PA6/CNT/GF laminates.[37] It was suggested that the CNTs acted as a sealing agent to create a network with the GF layers, forming a much tighter char than the fibers alone. A similar fire retardant mechanism involving the formation of a hybrid filler network that combines IF-WS_2 and GFs could be a suitable explanation for the observed OI enhancements.

Static Mechanical Properties. The results obtained from the room temperature tensile tests of the various laminates are displayed in Figure 6. For comparative purposes, data of neat iPP and binary iPP/IF-WS_2 nanocomposites are shown in the Supporting Information, Table S1. The Young's modulus (E) of iPP/GF laminate is ~3 GPa, about 2.5 fold that of the neat matrix, consistent with the stiffening effect found in short-GF reinforced iPP composites,[41] and rises only marginally upon further addition of the IF-WS_2, by ~10% at 4.0 wt % nanoparticle content (Figure 6a). A very similar trend is found for the tensile strength (σ_y), which increases by ~20% with the incorporation of 34 wt % GF to the matrix, whereas it changes only slightly for the ternary laminates, where the maximum increment is about 8% compared to iPP/GF. However, considerably larger increases were observed for the

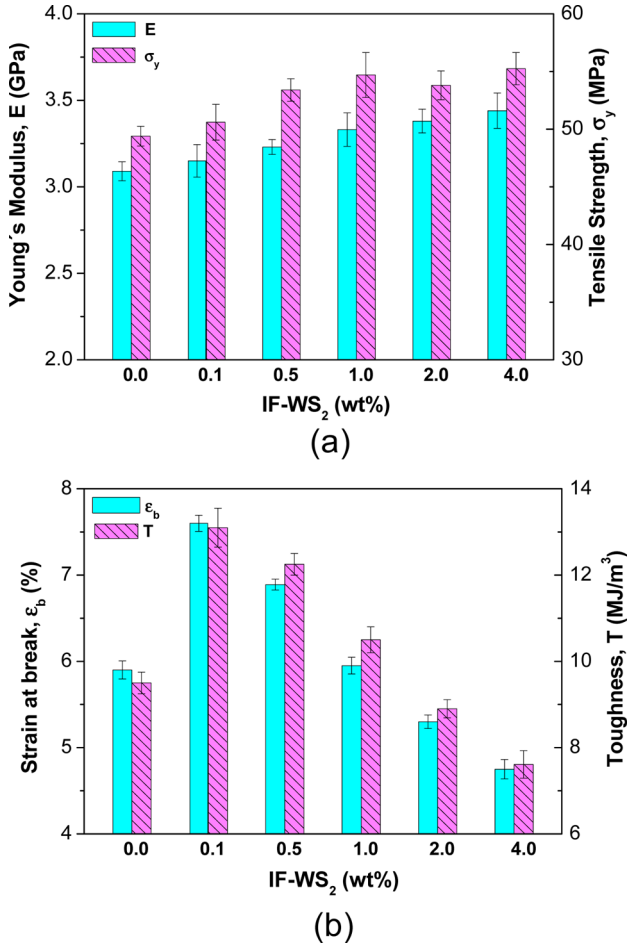

Figure 6. Comparison of the tensile properties of iPP/IF-WS_2/GF laminates with different nanoparticle loadings at 23 °C. (a) Young's modulus and tensile strength; (b) strain at break and toughness.

binary iPP/IF-WS_2 nanocomposites, being the highest improvements in E and σ_y of the matrix around 42 and 31%, respectively (see Table S1 in the Supporting Information). For multiscale composites, it is expected that the nanoscale reinforcement mostly influences the properties that are matrix-dominated; consequently, only a small increase is observed in the Young's modulus and tensile strength of the hybrids, since the tensile properties are more fiber-dominated. These results are consistent with the behavior reported for PEEK/CNT/GF[21] and PA6/nanoclay/GF laminates,[22] where E and σ_y of the binary thermoplastic/GF composites only improved marginally upon incorporation of the nanoscale fillers due to the dominating role of the fibers. Furthermore, it is also in agreement with the data reported by Rahman et al.[42] where the addition of nanoclay to PP/GF (30 wt %) had negligible effect on the tensile modulus and strength.

With regard to the strain at break (ε_b), which is around 32% for neat iPP (see Table S1 in the Supporting Information), a very strong reduction (more than 5-fold decrease) is found for the reference iPP/GF (Figure 6b), confirming that the fibers hinder the flow of the polymer chains, in agreement with previous works.[41] Focusing on the hybrid laminates, the trend observed is strongly dependent on the nanoparticle content, showing an increase up to 1.0 wt % loading and then decreasing moderately, by ∼19% at 4.0 wt % compared to iPP/GF. This indicates that higher amounts of IF-WS_2 also restrict the ductile flow of the matrix. This trend is in contrast to that reported for PEEK/CNT/GF[21] and PA6/nanoclay/GF laminates,[22] where ε_b systematically decreased upon addition of the nanofillers, ascribed to the presence of aggregates that generate stress concentrations at the filler−matrix interface, resulting in premature failure. Moreover, Rahman et al.[42] found around 50% reduction in tensile strain upon incorporation of 6.0 wt % nanoclay to PP/GF (30 wt %), also attributed to the poor nanoclay dispersion that strongly limits the plastic deformation of the matrix. The unexpected behavior observed in this work should be ascribed to the lubricant character and more uniform dispersion of the IF nanoparticles combined with their spherical shape that reduce the stress concentration sites, thereby improving the matrix ductility. However, for IF-WS_2 contents >1.0 wt %, a jammed hybrid network of micro- and nanofillers could be formed that acts more effectively as a barrier for the mobility of the polymer chains, thus restraining the ductile deformation. Analogously, the toughness (T) of the laminates (Figure 6b) measured as the area under the tensile curve, decreases ∼30% with the incorporation of the GF to iPP, ascribed to a ductile to brittle change in the facture mode.[41] T increases significantly at low IF-WS_2 loadings (i.e., by 35% at 0.1 wt % content compared to iPP/GF), whereas it drops moderately at concentrations higher than 1.0 wt % (around 20% decrease at 4.0 wt % loading). More importantly, the reduction in T upon incorporation of 4.0 wt % IF-WS_2 is considerably smaller than that reported for iPP[42] or PA6[22] hybrid composites incorporating 3.0 wt % nanoclay and 30 wt % GF, pointing out again the advantages of using the IF-WS_2 instead of conventional inorganic nanoparticles for improving the mechanical performance of thermoplastic composites.

On the other hand, the influence of the IF-WS_2 on the flexural properties of iPP/GF is shown in Figure 7a. Neat iPP has a flexural modulus (E_f) and flexural strength (σ_{FM}) of ∼1.7 GPa and 53 MPa (Supporting Information, Table S1), which show around 2.3 and 1.2 fold increase, respectively, with the inclusion of the GF. Further addition of increasing nanoparticle contents progressively raises both E_f and σ_{FM} of the laminates, with maximum increments compared to iPP/GF of 26 and 22%, respectively, at 2.0 wt % loading. The remarkable improvements attained upon incorporation of the IF-WS_2 that possess very high stiffness and strength[16] are ascribed to their reinforcement effect in the z-direction, since the flexural properties are more matrix-dominated than fiber-dominated. Moreover, the high nanoparticle surface area leads to a large contact area with the matrix, thereby increasing the interface, resulting in an efficient stress transfer. The stiffness enhancements are also associated with the nucleating effect of these nanoparticles on the iPP crystallization, because the crystalline regions are known to increase the modulus of semicrystalline polymers. The comparison of the results with those obtained for the binary iPP/IF-WS_2 nanocomposites (i.e., 21 and 15% increase in E_f and σ_{FM} of iPP upon incorporation of 2.0 wt % loading, Table S1 in the Supporting Information) reveals a synergistic effect of both fillers on enhancing the flexural properties of the matrix. The combination of GF and IF-WS_2 provides a very effective reinforcement to carry the load during the flexural deformation of the laminates. Analogous trend has been reported for vinyl ester/nanoclay/GF[43] and PP/nanoclay/GF,[39] where the increments in E_f and σ_{FM} attained in the hierarchical composites were significantly larger than those found for the corresponding binary samples. Interestingly, both the modulus and strength exhibit a maximum at a critical IF-

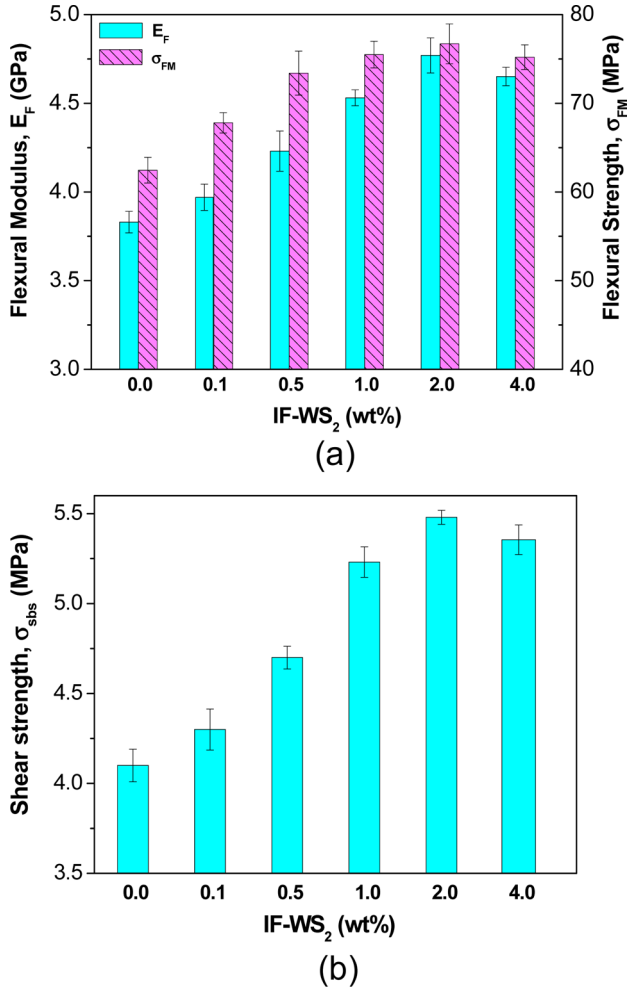

Figure 7. (a) Flexural modulus and flexural strength of iPP/IF-WS_2/GF laminates at 23 °C. (b) Short beam shear strength (σ_{sbs}) of the different laminates.

WS_2 concentration of 2.0 wt %; the incorporation of higher nanoparticle contents does not provide additional property improvements. This behavior should be related to the degree of crystallinity of the laminates (Table 1): X_c increases up to 2.0 wt % loading and then remains approximately constant. A similar phenomenon has been described for PP/nanoclay/GF,[39] where the optimal σ_{FM} was achieved at 6 wt % nanoclay content, while at higher loading the strength decreased due to a stress concentrating effect. It should be noted that, comparing similar loadings, the enhancements in the flexural properties achieved upon addition of the IF-WS_2 to iPP/GF are larger than those reached with other nanofillers such as SiO_2,[34] ZnO[23] or clay,[39] which makes them ideal candidates to reinforce polymeric materials for specific structural applications without the need for modifiers or compatibilizing agents. Furthermore, this approach enables to achieve similar property enhancements than those attained in conventional iPP/GF laminates using lower amount of fiber, which in turn leads to a composite weight reduction. Taking into account that the IF-WS_2 are relatively cheap nanofillers easily synthesized by a reaction of tungsten oxide with molecular hydrogen and hydrogen sulfide, and the very low nanoparticle content required to attain noticeable improvements in mechanical properties, it is envisaged that the replacement of part of the GF by a small amount of IF-WS_2 will be cost-effective.

The interlaminar shear strength (ILSS) is one of the most important parameters in determining the ability of a composite material to resist delamination damage. The ILSS of fiber-reinforced laminates gives information about the strength of the fiber/matrix interfacial adhesion. Figure 7b presents the short-beam shear strength (σ_{sbs}) values for the various laminates at 23 °C. A progressive rise in σ_{sbs} is observed with increasing nanoparticle loading up to 2.0 wt %, being the maximum increment about 33% in comparison to the reference iPP/GF. This trend is qualitatively similar to that described above for σ_{FM}, indicating that the flexural strength is governed by the interlaminar properties that are in turn influenced by the amount of nanoparticles at the interlayers. Qualitatively analogous phenomenon of shear strength improvement has been reported for hierarchical laminates incorporating nanoclays[44] or nanotubes.[20] The significant σ_{sbs} increment observed in this work is attributed to the very homogeneous dispersion of the nanoparticles, hence they could effectively hinder the crack growth within the matrix region, thereby increasing delamination resistance.

Thermomechanical Properties. The effect of the IF-WS_2 nanoparticles on the dynamic mechanical performance of iPP/GF was explored by dynamic mechanical analysis (DMA), which gives information about the viscoelastic behavior of the matrix, showing the changes in stiffness and the relaxation processes that take place as a function of temperature. Figure 8a plots the storage modulus (E') at the frequency of 1 Hz vs temperature for the various laminates, and the thermomechanical data extracted from the curves are tabulated in Table 2. A decreasing trend in E′ over the whole temperature range is observed: E′ of all the samples falls sharply from −10 to 50 °C, region associated with the relaxation of the amorphous phase (glass transition), while decreases only slightly at temperatures above 70 °C. E′ of iPP/GF laminate at 25 °C is about 2.6 GPa, a 1.7 fold increment in relation to that of neat iPP.[18] As can be observed in the inset of Figure. 8a, the addition of 0.1−4.0 wt % IF-WS_2 results in E' increases in the range of 11−36% compared to the reference laminate. This behavior is related to the nucleating effect of the nanoparticles, as discussed previously, combined with an effective reinforcement effect arising from a very homogeneous nanoparticle dispersion. In general, E′ rises with increasing nanoparticle loading in the whole temperature range, albeit the reinforcement effect is more pronounced at temperatures below T_g (Table 2). Thus, at −100 °C the addition of 4.0 wt % IF-WS_2 leads to an E' increase of around 27% compared to iPP/GF, whereas at 100 °C the relative increment is reduced to 13%. Analogous behavior has been described for PP/nanoclay/GF composites,[42] where significant E' enhancements were found at low temperatures whereas the differences in modulus among the samples became insignificant at temperatures above T_g. On the other hand, the E′ improvements reported for the binary iPP/IF-WS_2 nanocomposites[18] were smaller, about 20% at 4.0 wt % loading compared to neat iPP. Thus, it seems that a synergistic effect took place by incorporating nanoparticles into iPP/GF, leading to a higher stiffness than that expected due solely to the change in the matrix modulus.

The evolution of tan δ (ratio of the loss to storage modulus) as a function of temperature is shown in Figure 8b. The peak in tan δ (at ∼6 °C for iPP[18]) corresponds to the glass transition (T_g). iPP/GF laminate shows a T_g value of around 3 °C, slightly lower than that of the neat matrix, suggesting increased mobility of the amorphous regions in the composite compared

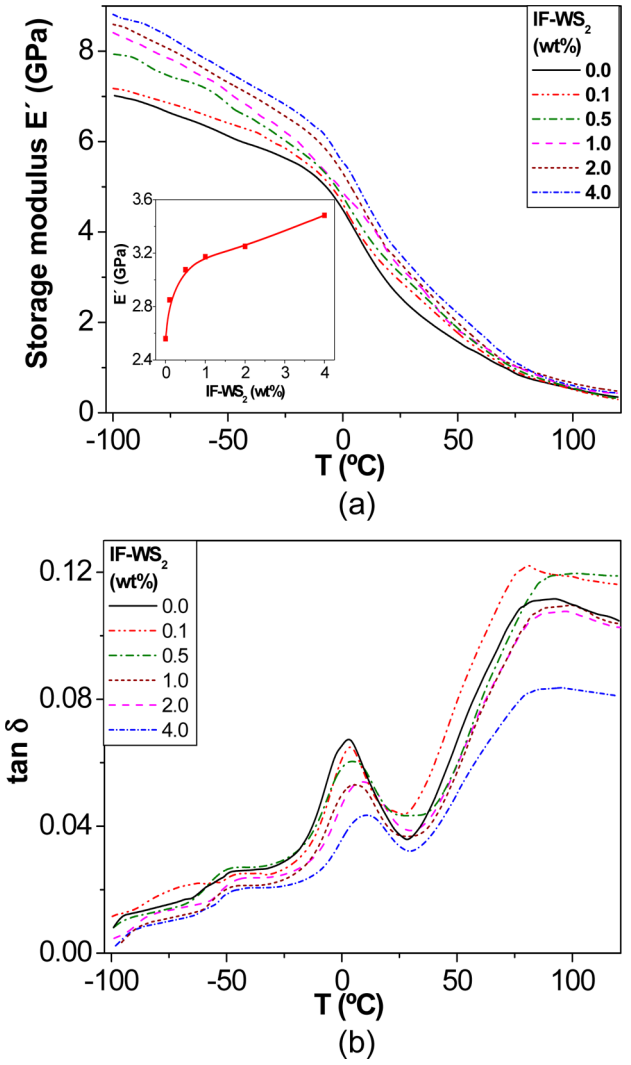

Figure 8. (a) Storage modulus E' and (b) tan δ curves as a function of temperature for iPP/IF-WS_2/GF laminates. The inset in a shows the room-temperature E' vs nanoparticle loading.

Table 2. Thermomechanical Data for iPP/IF-WS_2/GF Laminates[a]

IF-WS_2 content (wt%)	T_g (°C)	E'_{-100} (GPa)	E'_{25} (GPa)	E'_{100} (GPa)	tan δ_{max} ($\times 10^{-2}$)	tan δ_{width} (°C)	HDT (°C)
0.0	2.7	7.01	2.56	0.52	6.73	21.0	119
0.1	3.5	7.18	2.85	0.52	6.48	18.5	133
0.5	4.9	7.94	3.08	0.54	6.04	22.8	139
1.0	5.7	8.39	3.17	0.57	5.30	23.5	148
2.0	8.5	8.60	3.25	0.62	5.41	24.4	152
4.0	10.6	8.92	3.48	0.59	4.35	24.9	150

[a] E', storage modulus; T_g, glass transition temperature; tan δ_{max}, tan δ maximum value; tan δ_{width}, width at half maximum of tan δ peak; HDT, heat distortion temperature.

to the pure polymer. Clearly, T_g of the hybrid composites rises progressively with increasing IF-WS_2 loading, by up to 8 °C at 4.0 wt % in comparison to the reference laminate (Table 2). This indicates that the nanoparticles restrict the mobility of the matrix chains, which is reflected in higher T_g values. This behavior is in contrast to that reported for iPP/nanoclay/GF composites,[42] where the T_g was hardly altered by the presence of GF and nanoclay. The difference could be ascribed to the improved dispersion of the IF-WS_2 in comparison to the nanoclay, hence the spherical nanoparticles act more effectively as a barrier for the mobility of the chain segments in the amorphous region. Nevertheless, T_g of the binary iPP/IF-WS_2 nanocomposites was similar to that of the neat polymer,[18] suggesting a cooperative effect of both fillers on restricting polymer chain mobility, as discussed previously. The magnitude of tan δ peak is indicative of the filler−matrix interactions. In comparison with iPP/GF, the height of tan δ peak decreases gradually with increasing IF-WS_2 content, by up to 35% at 4.0 wt % loading (Table 2), which indicates an improvement in the interfacial adhesion of the composites. The incorporation of both reinforcements has a strengthening effect, leading to a lower degree of molecular motion hence lower damping characteristics, in agreement with the behavior reported for other GF-reinforced hierarchical composites.[21] It should also be noted that the width of tan δ peak becomes broader with increasing nanoparticle loading, phenomenon that can be interpreted as increased nanofiller-iPP interactions, and is another indication of the larger nanoparticle−matrix interfacial area. The IF-WS_2 and GF perturb the relaxation of the neighbor polymer chains, which would behave differently from those situated in the bulk matrix, resulting in a wider maximum. The aforementioned effect was also observed in iPP/IF-WS_2 nanocomposites,[18] attributed to a more inhomogeneous amorphous phase in the composites in relation to the pure matrix.

The heat distortion temperature (HDT) is a measure of the upper boundary for the dimensional stability of a material under a particular load and temperature, and is a critical parameter for product design, widely used in automotive applications. High HDT value is desirable to attain better performance during high-temperature service conditions. Both the presence of fibers and the inclusion of hard nanofillers such as clay[45] or CNTs[46] have been reported to enhance the HDT of thermoplastic polymers. The HDT data for the various laminates are collected in Table 2. The HDT of iPP/GF is 119 °C, about 1.8 fold higher than that of the neat matrix. The incorporation of increasing IF-WS_2 loadings leads to a progressive raise in this temperature up to 2.0 wt %, with a maximum increment of around 28% compared to the reference laminate, while it remains approximately constant at higher nanoparticle concentration. This trend is qualitatively similar to that described previously for the flexural modulus and strength, since the measurements were performed in three-point bending mode. Several factors are known to influence the HDT of polymeric materials, including the stiffness, the degree of crystallinity and the T_g.[47] These three parameters increase upon addition of the IF-nanoparticles, hence they positively contribute to enhance the HDT of the hierarchical laminates. Both the reinforcing effect and X_c reach a maximum at 2.0 wt % IF-WS_2, while the T_g rises steadily with the nanoparticle content. Therefore, the stiffness and crystallinity enhancements seem to prevail, resulting in an optimum HDT increment at 2.0 wt % loading. Qualitatively analogous behavior of HDT improvement has been reported for PA6/GF (30 wt %) composites upon addition of 3 wt % nanoclay,[22] whereas the incorporation of 0.1−4.0 wt % CNTs hardly modified the HDT of PA6/GF (49 wt %) laminates.[37] It is important to highlight that the HDT increments found for the iPP-based hybrid laminates are larger than those attained in the binary iPP/IF-WS_2 nanocomposites (i.e., about 11, 15, 24, 22, and 25% at 0.1,

0.5, 1.0, 2.0, and 4.0 wt % nanoparticle content, respectively), hinting toward the existence of a synergistic effect of both micro- and nanofillers on enhancing this thermomechanical property. This is consistent with the aforementioned synergetic behavior found for the flexural properties, the level of crystallinity and the T_g. Overall, the experimental data demonstrate that multiscale iPP/IF-WS_2/GF laminates are very suitable for engineering applications like transport industries.

4. CONCLUSIONS

iPP/IF-WS_2/GF laminates were successfully fabricated via melt-blending and hot-press processing without the aid of any modifier or compatibilizing agent. The effect of IF-WS_2 content on the morphology, viscosity, thermal and mechanical behavior of the hybrid composites was analyzed. A strong drop in viscosity was found upon addition of the nanoparticles due to their lubricant effect, resulting in a very uniform dispersion within the matrix. The nanoparticles acted as nucleating agents, raising the crystallization temperature and crystallinity of iPP. Further, they strongly improved matrix-dominated mechanical properties (e.g., flexural and interlaminar shear strength), whereas they slightly influenced the tensile properties because of the fiber-dominating effect. Significant enhancements in thermomechanical properties (e.g., glass transition, T_g, and heat distortion temperature, HDT) were also observed. The laminates exhibited quasi-isotropic thermal conductivity behavior; both the in-plane and transverse conductivities increased with the IF-WS_2 concentration. Laminates with 2.0 wt % IF-WS_2 displayed the optimum overall performance. The results reveal the existence of synergistic effects between the micro- and nanoscale fillers on enhancing the stiffness, strength, crystallinity, thermal stability, T_g, and HDT of the matrix. This study demonstrates the feasibility of developing advanced GF-reinforced iPP laminates for a wide range of technological applications, in particular for the transport industries, by incorporating small amounts of IF-WS_2. The approach used in this work is a simple, versatile, scalable, economic, and environmentally friendly strategy that can be applied to the manufacture of diverse hierarchical thermoplastic-based composites.

■ ASSOCIATED CONTENT

Supporting Information

Mechanical properties of neat iPP and binary iPP/IF-WS_2 nanocomposites are provided. This material is available free of charge via the Internet at http://pubs.acs.org/

■ AUTHOR INFORMATION

Corresponding Author

*E-mail: adiez@ictp.csic.es.

Notes

The authors declare no competing financial interest.

■ ACKNOWLEDGMENTS

Financial support from the Ministerio de Ciencia e Innovación (MICINN, Project MAT2010-21070-C02-01) is gratefully acknowledged. M.N. acknowledges the Ministerio de Economía y Competitividad (MINECO) for a Ramon y Cajal Research Senior fellowship. A.D. thanks the CSIC for a JAE postdoctoral contract.

■ REFERENCES

(1) Marsh, G. *Mater. Today* **2003**, *6*, 36−43.
(2) Diez-Pascual, A. M.; Naffakh, M. *Polymer* **2012**, *53*, 2369−2378.
(3) Seo, M. K.; Lee, J. R.; Park, S. J. *Mater. Sci. Eng., A* **2005**, *404*, 79−84.
(4) Shi, D.; Yang, J. H.; Yao, Z. H.; Wang, Y.; Huang, H. L.; Jing, W. *Polymer* **2001**, *42*, 5549−5557.
(5) Mohanty, S.; Nayak, S. K.; Verma, S. K.; Tripathy, S. S. *J. Reinf. Plast. Compos.* **2004**, *23*, 625−637.
(6) Kim, Y. F.; Choi, C. N.; Kim, Y. D.; Lee, Y. K.; Lee, M. S. *Fiber Polym.* **2004**, *5*, 270−274.
(7) Shariatpanahi, H.; Sarabi, F.; Mirali, M.; Hemmati, M.; Mahdavi, F. *J. Appl. Polym. Sci.* **2009**, *113*, 922−926.
(8) Thio, Y. S.; Argon, A. S.; Cohen, R. E.; Weinberg, M. *Polymer* **2002**, *43*, 3661−3674.
(9) Vassiliou, A.; Vikiaris, D.; Pavlidou, E. *Macromol. React. Eng.* **2007**, *1*, 488−501.
(10) Naffakh, M.; López, V.; Zamora, F.; Gómez, M. A. *Soft Materials* **2010**, *8*, 407−425.
(11) Manchado, M. A. L.; Valentini, L.; Biagiotti, J.; Kenny, J. M. *Carbon* **2005**, *43*, 1499−1505.
(12) Haque, M. A.; Mina, M. F.; Alam, A. K. M. M.; Rahman, M. J.; Bhuiyan, M. A. H.; Asano, T. *Polym. Compos.* **2012**, *33*, 1094−1104.
(13) Meng, M.-R.; Dou, Q. *J. Macromol. Sci. B: Phys.* **2009**, *48*, 213−225.
(14) Gao, X. Q.; Xu, J.; Chen, Z. C.; Deng, C.; Shen, K. Z. *Polym. Int.* **2008**, *57*, 23−27.
(15) Altan, M.; Yildirim, H.; Uysal, A. *J. Sci. Technol.* **2011**, *1*, 25−30.
(16) Naffakh, M.; Díez-Pascual, A. M.; Marco, C.; Ellis, G.; Gomez-Fatou, M. A. *Prog. Polym. Sci.* **2013**, *38*, 1163−1231.
(17) Naffakh, M.; Díez-Pascual, A. M.; Marco, C.; Gómez, M. A.; Jiménez, I. *J. Phys. Chem. B* **2010**, *114*, 11444−11453.
(18) Naffakh, M.; Martin, Z.; Fanegas, N.; Marco, C.; Gómez, M. A.; Jiménez, I. *J. Polym. Sci. B: Polym. Phys.* **2007**, *45*, 2309−2321.
(19) Tong, L.; Mouritz, A. P.; Bannister, M. In *3D Fibre Reinforced Polymer Composites*; Elsevier Science: Oxford, U.K., 2002.
(20) Ashrafi, B.; Díez-Pascual, A. M.; Johnson, L.; Genest, M.; Hind, S.; Martinez-Rubi, Y.; González-Domínguez, J. M.; Martínez, M. T.; Simard, B.; Gómez-Fatou, M. A.; Johnston, A. *Composites, Part A* **2012**, *43*, 1267−1279.
(21) Díez-Pascual, A. M.; Ashrafi, B.; Naffakh, M.; González-Domínguez, J. M.; Johnston, A.; Simard, B.; Martinez, M. T.; Gomez-Fatou, M. A. *Carbon* **2011**, *49*, 2817−2833.
(22) Wu, S.-H.; Wang, F.-Y.; Ma, C.-C. M.; Chang, W.-C.; Kuo, C.-T.; Kuan, H.-C.; Chen, W.-J. *Mater. Lett.* **2001**, *49*, 327−333.
(23) Cui, Y.-H.; Wang, X.-X.; Li, Z.-Q.; Tao, J. *J. Vinyl Addit. Technol.* **2010**, *16*, 189−194.
(24) Romero-Guzmán, M. E.; Romo-Uribe, A.; González, A. E.; Cruz-Silva, R. *J. Appl. Polym. Sci.* **2008**, *109*, 2207−2218.
(25) Kim, S. H.; Ahn, S. H.; Hirai, T. *Polymer* **2003**, *44*, 5625−5634.
(26) Im, S. S.; Chung, S. C.; Hahm, W. G.; Oh, S. G. *Macromol. Res.* **2002**, *10*, 221−229.
(27) Romero-Guzmán, M. E.; Romo-Uribe, A.; Zárate-Hernández, B. M.; Cruz-Silva, R. *Rheol. Acta* **2009**, *48*, 641−652.
(28) Tuteja, T.; Mackay, M. E.; Hawker, C. J.; Van Horn, B. *Macromolecules* **2005**, *38*, 8000−8011.
(29) Heo, Y.; Larson, R. G. *J. Rheol.* **2005**, *49*, 1117−1128.
(30) Batchelor, G. K. *J. Fluid Mech.* **1970**, *41*, 545−570.
(31) Diez-Pascual, A. M.; Naffakh, M.; Marco, C.; Ellis, G. *J. Phys. Chem. B* **2012**, *116*, 7959−7969.
(32) Teng, C.-C.; Ma, C.-C. M.; Huang, Y.-W.; Yuen, S.-M.; Weng, C.-C.; Chen, C.-H.; Su, S.-F. *Compos., Part A* **2008**, *39*, 1869−1875.
(33) Majid, M.; Hassan, E.-D.; Davoud, A.; Saman, M. *Compos., Part B* **2011**, *42*, 2038−2046.
(34) Jacob, S.; Suma, K. K.; Mendaz, J. M.; George, A.; George, K. E. *Macromol. Symp.* **2009**, *277*, 138−143.
(35) Dasgupta, A.; Agarwal, R. K.; Bhandarkar, S. M. *Compos. Sci. Technol.* **1996**, *56*, 209−223.

(36) Díez-Pascual, A. M.; Naffakh, M.; Gómez-Fatou, M. A. *Mater. Chem. Phys.* **2011**, *130*, 126−133.
(37) Shen, Z.; Bateman, S.; Wu, D. Y.; McMahon, P.; Dell'Olio, M.; Gotama, J. *Compos. Sci. Technol.* **2009**, *69*, 239−244.
(38) Nan, C.-W.; Liu, G.; Lin, Y.; Li, M. *Appl. Phys. Lett.* **2004**, *85*, 3549−3551.
(39) Rahman, N. A.; Hassan, A.; Yahya, R.; Lafia-Araga, R. A.; Hornsby, P. R. *J. Reinf. Plast. Compos.* **2012**, *31*, 269−281.
(40) van Krevelen, D. W. *Polymer* **1975**, *16*, 615−620.
(41) Flores, O.; Romo-Uribe, A.; Romero-Guzmán, M. E.; González, A. E.; Cruz-Silva, R.; Campillo, B. *J. Appl. Polym. Sci.* **2009**, *112*, 934−941.
(42) Rahman, N. A.; Hassan, A.; Yahya, R.; Lafia-Araga, R. A.; Hornsby, P. R. *J. Reinf. Plast. Compos.* **2012**, *31*, 1247−1257.
(43) Chandradass, J.; Ramesh, K. M.; Velmurugan, R. *J. Reinf. Plast. Compos.* **2008**, *27*, 1585−1601.
(44) Daud, W.; Bersee, H. E. N.; Picken, S. J.; Beukers, A. *Compos. Sci. Technol.* **2009**, *69*, 2285−2292.
(45) Kojima, Y.; Usuki, A.; Kawasumi, M.; Okada, A.; Fukushima, Y.; Kirauchi, T. *J. Mater. Res.* **1993**, *8*, 1185−1189.
(46) Pascual, J.; Peris, F.; Boronat, T.; Fenollar, O.; Balart, R. *Polym. Eng. Sci.* **2011**, *52*, 733−740.
(47) McKeen, L. W. In *Effect of Temperature and other Factors on Plastics and Elastomers*, 2nd ed.; William Andrew: Norwich, NY, 2007.